Flutter of Flat Plates with Partially Clamped Edges in the Low Supersonic Region

E. F. E. Zeydel* and D. R. Kobett†
Midwest Research Institute, Kansas City, Mo.

A supersonic flutter analysis of an infinite span plate, which is separated into an array of rectangular panels, is presented. The region between Mach 1 and $2^{1/2}$ is of specific interest, and linearized three-dimensional aerodynamic theory is applied. The elastic behavior of the configuration is described by small deflection theory. The partially clamped edge condition is obtained by introducing a torsional restraint proportional to the first derivative of the transverse deflection along the normal to the edge. Numerical results are given in terms of characteristic panel flutter parameters. The effects of Mach number, aspect ratio, number of panels in the chordwise direction, panel material, and altitude are examined.

Nomenclature

$A_{m,\,t}$ = coefficient in expansion of chordwise deflection function
a = chord of one panel (Fig. 1)
B_u = coefficient in expansion of spanwise deflection function
b = span of one panel
$C_{m,\,l^*}, D_{m,\,l^*}$ = coefficients in chordwise deflection function [Eq. (13)]
c_∞ = sound velocity
D = $Eh^3/12(1-\nu^2)$ = flexural rigidity of panel
E = modulus of elasticity
f_m = defined by (13)
f^* = defined by (14)
g = structural damping coefficient
h = panel thickness
$I_{m,\,m^*,\,u}$ = defined by (23)
$J_{m,\,m^*}$ = defined by (17)
j^2 = -1
K = kM/β^2
$K_{m,\,m^*}$ = defined by (17)
k = $\omega a/U$ = reduced frequency
k^* = integer denoting specific spanwise panel
L = number of panels in chordwise direction
l, l^* = integers denoting specific chordwise panels
M = Mach number
m, m^* = chordwise modal number
n, n^* = spanwise modal number
P_u = defined by (20)
p^* = defined by (5)
p = perturbation pressure at upper surface of panel
q = $\rho U^2/2$ = dynamic pressure
$q_{m,\,n}$ = generalized coordinate of m, nth mode shape
$R_{m,\,m^*}$ = defined in (23)
S = defined by (17)
s = $a/b = 1/AR$ = inverse of aspect ratio of panel
T = defined by (17)
t = time
U = freestream velocity
w = transverse displacement of panel (in the z direction)
x, y, z = reference coordinate system
α = $\tau^3 E/12\rho c_\infty^2(1-\nu^2)$
β = $(M^2-1)^{1/2}$
Γ = defined by (20)
γ_m = frequency for chordwise deflection function
γ^* = frequency for spanwise deflection function
ϵ_x = coefficient expressing stringer restraint against rotation
ϵ_y = coefficient expressing rib restraint against rotation
η = local coordinate defined by (10)
θ = local coordinate defined by (7)
μ = $\tau\rho_s/\rho$
ν = Poisson's ratio
ξ = nondimensional chordwise coordinate
ρ = mass air density
ρ_s = mass density of panel
τ = h/a = nondimensional panel thickness ratio
Φ_m = chordwise deflection function
$\Phi_{m,\,l^*}$ = defined by (7) and (8)
ψ_n = spanwise deflection function
φ = local coordinate defined by (27)
ω = frequency of vibration
$(\ )^{(i\xi)}$ = $\partial^i(\ )/\partial\xi^i$

Presented as Preprint 63-25 at the IAS 31st Annual Meeting, New York, January 20–23, 1963; revision received September 16, 1964. This paper is based on research supported by the Air Force Office of Scientific Research under Contract No. AF 49(638)-389.

* Head, Mathematical Analysis Section; now Professor of Aerospace Engineering, Georgia Institute of Technology. Associate Fellow Member AIAA.
† Associate Analyst. Member AIAA.

Introduction

In the development of design criteria to prevent the flutter of flat plates, it is desirable to consider the torsional stiffness of the supporting structure. This structure usually consists of ribs and stringers with torsional rigidity simulating boundary conditions somewhere between pinned and clamped. In general, these boundary conditions greatly influence the flutter instability characteristics of flat plates. Also, it has been shown in the literature (see Ref. 1, for instance) that the largest thickness ratios to prevent flutter are needed in the low supersonic region.

Practical configurations consist of an array of panels that extend in the chordwise as well as spanwise direction. Although these panels are not always similar in size and form, it is of interest to investigate the case of an array of identical rectangular panels.

In this paper, a supersonic flutter analysis of an infinite span plate, which is separated into an array of rectangular panels, is presented. Since the low supersonic region is of particular interest, linearized three-dimensional aerodynamic theory is applied. The torsional stiffness of the ribs and stringers is assumed to be proportional to the first derivative of the transverse deflection along the normal to the edges. The effects of Mach number, aspect ratio, number of panels in the chordwise direction, panel material, and altitude are examined in terms of characteristic panel flutter parameters.

Equations of Motion

Consider the array of rectangular panels shown in Fig. 1. The array extends to infinity in the spanwise direction and to

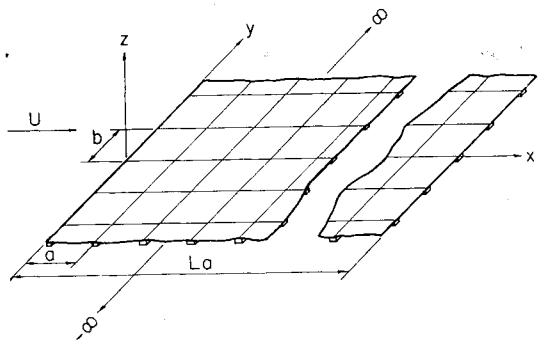

Fig. 1 Array of panels.

L panels in the chordwise direction. All panels are geometrically similar with length a and width b. At their edges, the panels are supported by a series of stringers (in the y direction) and ribs (in the x direction). The array is exposed to supersonic flow on the side $z > 0$.

From small deflection plate theory the equation of motion for the array is[1]

$$D\nabla^4 w + \rho_s h w^{(2t)} + p^*(x, y, t) = 0 \tag{1}$$

In Eq. (1), w is the transverse displacement in the z direction, D the plate bending stiffness, ρ_s the material density, h the thickness, and p^* the aerodynamic pressure of the air flow at the side $z > 0$.

It is convenient to introduce dimensionless variables x', y', etc., by writing

$$\begin{gathered} x = ax' \qquad y = by' \\ w = aw' \qquad p^* = \rho U^2 p^{*\prime} \qquad s = a/b \end{gathered} \tag{2}$$

where ρ is the air density and U is the forward velocity.

Dropping the primes in the ensuing discussion, Eq. (1) in dimensionless form becomes

$$w^{(4x)} + 2s^2 w^{(2x,\ 2y)} + s^4 w^{(4y)} + [(\rho_s h a^4)/D] w^{(2t)} + [(\rho U^2 a^3)/D] p^*(x, y, t) = 0 \tag{3}$$

The solution of Eq. (3) can readily be obtained by the Ritz-Galerkin method. Because the motion at flutter is harmonic, let

$$w = e^{i\omega t} \sum_{m,\,n} q_{m,\,n} \Phi_m(x) \psi_n(y) \tag{4}$$

and

$$p^*(x, y, t) = e^{i\omega t} p(x, y) \tag{5}$$

Substitute (4) and (5) in (3); then multiply through by $\Phi_{m^*}(x)\psi_{n^*}(y)$ and integrate across the length and width of the array of panels. The resulting equations are

$$\begin{aligned} \sum_{m,\,n} q_{m,\,n} \Bigg\{ & \int_0^L \Phi_m^{(4x)} \Phi_{m^*} dx \int_{-\infty}^{+\infty} \psi_n \psi_{n^*} dy + \\ & 2s^2 \int_0^L \Phi_m^{(2x)} \Phi_{m^*} dx \int_{-\infty}^{+\infty} \psi_n^{(2y)} \psi_{n^*} dy + \\ & s^4 \int_0^L \Phi_m \Phi_{m^*} dx \int_{-\infty}^{+\infty} \psi_n^{(4y)} \psi_{n^*} dy - \\ & \left[\frac{(\rho_s h a^4 \omega^2)}{D}\right] \int_0^L \Phi_m \Phi_{m^*} dx \int_{-\infty}^{+\infty} \psi_n \psi_{n^*} dy \Bigg\} + \\ & \left[\frac{(\rho U^2 a^3)}{D}\right] \int_0^L \int_{-\infty}^{+\infty} p \Phi_{m^*} \psi_{n^*} dy dx = 0 \end{aligned} \tag{6}$$

Next, a suitable set of functions, $\Phi_m(x)$ and $\psi_n(y)$, must be chosen to satisfy the boundary conditions of the array of panels. Rather than satisfy the exact boundary conditions[2] for the skin-rib-stringer configuration, which are complex, in this paper the ribs and stringers are assumed to be infinitely rigid in bending. The torsional rigidity of the ribs and stringers is represented by an elastic restraint against rotation with the basic property that the rotation at one point does not influence the rotation at any other point. Consequently, the transverse deflections along the edges of the panels are zero, whereas the bending moments along the edges are proportional to the slope perpendicular to the edges.

In the formulation of the boundary conditions along the stringers, it is convenient to introduce a dimensionless, local coordinate and deflection

$$\theta = x - (l^* - 1) \qquad l^* - 1 \leq x \leq l^* \tag{7}$$

$$\Phi_m = \Phi_{m,\ l^*}(\theta) \qquad l^* = 1, 2, \ldots, L \tag{8}$$

Taking the elastic restraint against rotation at the leading and trailing edge stringers twice as small as the elastic restraints at the intermediate stringers, the boundary and compatibility conditions become

$$\Phi_{m,\ l^*}(0) = \Phi_{m,\ l^*}(1) = 0 \qquad l^* = 1, 2, \ldots, L \tag{9a}$$

$$\Phi_{m,\ l^*-1}{}^{(\theta)}(1) = \Phi_{m,\ l^*}{}^{(\theta)}(0) \qquad l^* = 2, 3, \ldots, L \tag{9b}$$

$$\Phi_{m,\ l^*-1}{}^{(2\theta)}(1) + \epsilon_x \Phi_{m,\ l^*-1}{}^{(\theta)}(1) = \Phi_{m,\ l^*}{}^{(2\theta)}(0) - \epsilon_x \Phi_{m,\ l^*}{}^{(\theta)}(0) \qquad l^* = 2, 3, \ldots, L \tag{9c}$$

$$\Phi_{m,\ 1}{}^{(2\theta)}(0) = \epsilon_x \Phi_{m,\ 1}{}^{(\theta)}(0) \tag{9d}$$

$$\Phi_{m,\ L}{}^{(2\theta)}(1) = -\epsilon_x \Phi_{m,\ L}{}^{(\theta)}(1) \tag{9e}$$

where ϵ_x is a coefficient expressing the stringers restraint. Similarly, with

$$\eta = y - (k - 1) \qquad k - 1 \leq y \leq k \tag{10}$$

$$\psi_n = \psi_{n,\ k}(\eta) \qquad k = -\infty, \ldots, +\infty \tag{11}$$

the boundary and compatibility conditions at the ribs become

$$\psi_{n,\ k}(0) = \psi_{n,\ k}(1) \tag{12a}$$

$$\psi_{n,\ k-1}{}^{(\eta)}(1) = \psi_{n,\ k}{}^{(\eta)}(0) \tag{12b}$$

$$\psi_{n,\ k-1}{}^{(2\eta)}(1) + \epsilon_y \psi_{n,\ k-1}{}^{(\eta)}(1) = \psi_{n,\ k}{}^{(2\eta)}(0) - \epsilon_y \psi_{n,\ k}{}^{(\eta)}(0) \qquad k = -\infty, \ldots, +\infty \tag{12c}$$

where ϵ_y is a coefficient expressing the rib restraint.

To satisfy these conditions, it is appropriate to take for $\Phi_m(x)$ and $\psi_n(y)$ the deflection mode shapes associated with the natural frequencies of beams having the same boundary conditions as (9) and (12), respectively.

The natural frequencies and mode shapes of a continuous beam resting on an arbitrary number of equally spaced supports are given by Miles in Ref. 3. An extension of these analyses shows that the deflection functions $\Phi_m(x)$ that satisfy (9) can be written in the form

$$\Phi_{m,\ l^*} = C_{m,\ l^*} f_m(\theta) + D_{m,\ l^*} f_m(1 - \theta) \tag{13}$$

where $f_m(\theta) = \sinh \gamma_m \sin \gamma_m \theta - \sin \gamma_m \sinh \gamma_m \theta$. The derivation of (13) is given in the Appendix of Ref. 7.

The fact that the span of the array is infinite gives rise to some complication in the selection of $\psi_n(y)$. As shown by Miles, the frequency spectrum of a continuous beam on equally spaced supports becomes continuous over specific frequency intervals when the number of beam sections becomes infinite. It is expected, however, that the coupling between chordwise modes is more important than the coupling between spanwise modes, since the forward velocity is in the chordwise direction, and the coupling predominantly results from the aerodynamic forces. In the ensuing analysis, a specific spanwise deflection function is therefore introduced. An appropriate choice for $\psi_n(y)$ is the mode shape associated with the lowest natural frequency of a continuous beam on

equally spaced supports subject to the boundary conditions (12). Consequently, $\psi_n(y)$ becomes[7]

$$\psi_1(\eta) = (-1)^{k-1}[f^*(\eta) + f^*(1 - \eta)] \tag{14}$$

where $f^*(\eta) = \sinh \gamma^* \sin\gamma^*\eta - \sin\gamma^* \sinh \gamma^*\eta$.

Note that this function is periodic with half-period of unity, so that it will suffice to take, for the limits of the spanwise integrals in Eq. (6), 0 and 1, rather than $-\infty$ and $+\infty$.

Define the dimensionless parameters

$$\mu = \tau\rho_s/\rho \tag{15}$$

$$\alpha = \tau^3 E/12\rho c_\infty^2(1 - \nu^2) \tag{16}$$

where

$\tau = h/a$

c_∞ = speed of sound

E = modulus of elasticity

ν = Poisson's ratio

In addition, let

$$J_{m,\,m^*} = \int_0^L \Phi_m\Phi_{m^*}dx \qquad K_{m,\,m^*} = \int_0^L \Phi_m{}^{(2x)}\Phi_{m^*}dx$$

$$S = \int_0^1 \psi_1{}^2dy \qquad T = \int_0^1 \psi_1{}^{(2y)}\psi_1 dy \tag{17}$$

which can be obtained readily from (13) and (14). These integrals are evaluated in the Appendix of Ref. 7.

Substitution of (15–17) in (6) yields the set of equations

$$\sum_m q_m \left\{\alpha[(\gamma_m{}^4 + s^4\gamma^{*4})J_{m,\,m^*}S + 2s^2K_{m,\,m^*}] - \mu k^2M^2J_{m,\,m^*}S + M^2\int_0^L\int_0^1 p\Phi_{m^*}\psi_1 dydx\right\} = 0 \tag{18}$$

in which $k = \omega a/U$ and M is Mach number.

It is of interest to note that, although $J_{m,\,m^*}$ is a diagonal matrix, $K_{m,\,m^*}$ is a full matrix if $\epsilon_x \neq 0$, so that there is elastic coupling between the coordinates q_m.

The aerodynamic integral will be defined in the next section.

Aerodynamic Integral

Since the region between Mach 1 and $2^{1/2}$ is of particular interest, the aerodynamic pressures are obtained from linearized, three-dimensional aerodynamic theory. From the analysis of Luke and St. John,[4] the perturbation pressure at the upper surface for harmonic motion, sinusoidal spanwise deflection and chordwise deflection $\Phi_m(x)$, can be written in the dimensionless form

$$p_u = \frac{1}{\beta}\sin u\pi y\left[\Phi_m{}^{(x)} + jk\left(\frac{M^2 - 2}{\beta^2}\right)\Phi_m + \int_0^x P_u(\xi)\Phi_m(x - \xi)d\xi\right] \tag{19}$$

where

$$P_u(\xi) = e^{-jKM\xi}\left[-\left(\frac{\Gamma_u{}^2}{2} + \frac{k^2}{\beta^4}\right)J_0(\Gamma_u\xi) + j\left(\frac{2k\Gamma_u}{\beta^2}\right)J_1(\Gamma_u\xi) + \left(\frac{\Gamma_u{}^2}{2}\right)J_2(\Gamma_u\xi)\right]$$

$$K = \frac{kM}{\beta^2} \qquad \Gamma_u{}^2 = K^2 + \left(\frac{u\pi s}{\beta^2}\right) \qquad \beta^2 = M^2 - 1 \tag{20}$$

and J_n are Bessel functions of the first kind.

It is therefore convenient to use a Fourier series representation for $\psi_1(y)$ and write

$$\psi_1(y) = \sum_u B_u \sin u\pi y \tag{21}$$

The aerodynamic integral in (18) then becomes

$$\int_0^L\int_0^1 p\Phi_{m^*}\psi_1 dydx = \frac{1}{\beta}\left\{R_{m,\,m^*}S + jk\left(\frac{M^2 - 2}{\beta^2}\right)J_{m,\,m^*}S\right\} + \frac{1}{2\beta}\sum_u B_u{}^2I_{m,\,m^*,\,u} \tag{22}$$

where

$$R_{m,\,m^*} = \int_0^L \Phi_m{}^{(x)}\Phi_{m^*}dx$$

$$I_{m,\,m^*,\,u} = \int_0^L\int_0^x P_u(\xi)\Phi_m(x - \xi)\Phi_{m^*}(x)d\xi dx \tag{23}$$

The integral $R_{m,\,m^*}$ can easily be obtained by substituting (13). To evaluate $I_{m,\,m^*,\,u}$, two procedures can be followed.

1) When L and m are small, it is expedient to approximate the Bessel functions in $P_u(\xi)$ by a sum of circular functions as in Ref. 4 so that

$$P_u(\xi) = \sum_{r=1}^q e^{-jKM\xi}\{a_r\cos\lambda_r\xi + jb_r\sin\lambda_r\xi\} \tag{24}$$

where

$$a_r = -(1/q)\{(k^2/\beta^4) + \Gamma^2\cos^2[(2r - 1)/4q]\pi\}$$

$$b_r = (2\Gamma k/q\beta^2)\cos[(2r - 1)/4q]\pi \tag{25}$$

$$\lambda_r = \Gamma\cos[(2r - 1)/4q]\pi$$

and to expand $\Phi_m(x)$ in a Fourier series with half-period L

$$\Phi_m(x) = \sum_t A_{m,\,t}\sin(t\pi/L)x \tag{26}$$

2) When L is large, however, it is more convenient to define, similarly to (7), the local coordinate

$$\varphi = \xi - (l - 1) \qquad l - 1 \leq \xi \leq l \tag{27}$$

Then, using (13) and (23),

$$I_{m,\,m^*,\,u} = \int_0^L P_u(\xi)\int_\xi^L \Phi_m(x - \xi)\Phi_{m^*}(x)dxd\xi = \left.\begin{aligned}&\sum_{l=1}^L \int_0^1 P_u(l - 1 + \varphi)G_{m,\,m^*,\,l}(\varphi)d\varphi + \\ &\sum_{l=1}^{L-1}\int_0^1 P_u(l - 1 + \varphi)H_{m,\,m^*,\,l}(\varphi)d\varphi\end{aligned}\right\} \tag{28}$$

where

$$G_{m,\,m^*,\,l}(\varphi) = \sum_{l^*=l}^L \int_\varphi^1 \Phi_{m,\,l^*-l+1}(\theta - \varphi)\Phi_{m^*,\,l^*}(\theta)d\theta$$

$$H_{m,\,m^*,\,l}(\varphi) = \sum_{l^*=l+1}^L \int_0^\varphi \Phi_{m,\,l^*-l}(1 + \theta - \varphi)\Phi_{m^*,\,l^*}(\theta)d\theta \tag{29}$$

The integrals in (29) can readily be obtained. Because of the appearance of P_u with shifted argument $(l - 1 + \varphi)$ in (28), however, it is simpler to evaluate these integrals numerically. For a more detailed evaluation of the preceding aerodynamic integrals, the reader is again referred to the Appendix of Ref. 7.

It is instructive to remark that the Fourier series expansion of $\Phi_m(x)$ can also be used for the evaluation of $J_{m,\,m^*}$, $K_{m,\,m^*}$, and $R_{m,\,m^*}$. Such a procedure is, however, not attractive because the series representation is less convergent in the higher derivatives and for larger values of m. Also, care

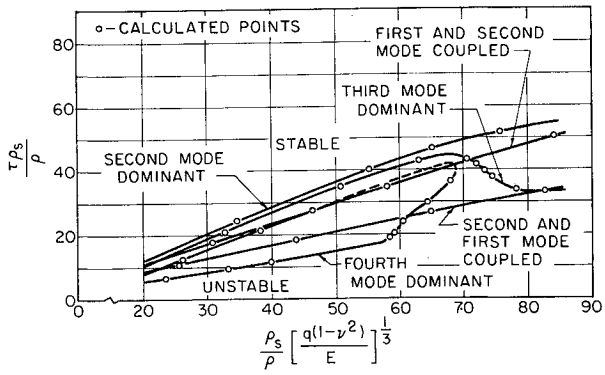

Fig. 2 Stability boundaries from four-mode analysis for flat panels with partially clamped edges, $M = 1.35$, $s = \frac{1}{4}$, $g = 0.01$, $L = 1$, $\epsilon = 1.0$.

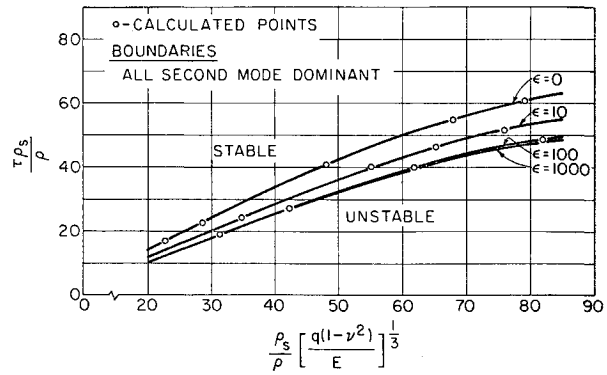

Fig. 4 Critical stability boundaries from four-mode analysis for flat panels with partially clamped edges, $M = 1.35$, $s = \frac{1}{4}$, $g = 0.01$, $L = 1$.

should be exercised since, in general, an infinite Fourier series cannot be differentiated term-by-term.[5]

Flutter Equations and Method of Solution

The flutter equations of motion follow from (18) and (22),

$$\sum_m q_m \Big\{ \alpha(1 + jg)[(\gamma_m{}^4 + s^4\gamma^{4*})J_{m,m^*}S + 2s^2K_{m,m^*}T] - \mu k^2M^2J_{m,m^*}S + \frac{M^2}{\beta}\left[R_{m,m^*}S + jk\left(\frac{M^2-2}{\beta^2}\right)J_{m,m^*}S\right] + \frac{M^2}{2\beta}\sum_u B_u{}^2I_{m,m^*,u}\Big\} = 0 \quad (30)$$

In (30), the stiffness terms are multiplied by $(1 + jg)$ to account for structural damping.

The condition for nontrivial solutions of (30) is that the determinant of the coefficients of q_m vanish. To satisfy this condition, α and μ are chosen to be free parameters. There fore, values of M, L, k, s, g, ϵ_x, and ϵ_y must be specified.

The procedure used for determining α and μ is as follows. The flutter determinant of (30) can be written as a polynomial in μ with complex coefficients that depend on α,

$$D(\mu) = a_0\mu^m + a_1\mu^{m-1} + \ldots + a_m \quad (31)$$

Because D should vanish and μ must be real, the flutter condition becomes

$$f(\mu) = \mu^m + (a_1/a_0)_R\mu^{m-1} + \ldots + (a_m/a_0)_R = 0$$
$$g(\mu) = (a_1/a_0)_I\mu^{m-1} + \ldots + (a_m/a_0)_I = 0 \quad (32)$$

Consequently, f and g should have a common root. The condition that two polynomials in one variable have a common root can be obtained from Euclid's algorithm.[6] Because f is of higher order in μ, it can be divided by g to give

$$f(\mu) = Q_0(\mu)g(\mu) + R_1(\mu) \quad (33)$$

where Q_0 is the quotient polynomial and R_1 is the remainder polynomial. Continuing the process by dividing g by R_1, etc, the following system of identities results:

$$\begin{aligned} g(\mu) &= Q_1(\mu)R_1(\mu) + R_2(\mu) \\ R_1(\mu) &= Q_2(\mu)R_2(\mu) + R_3(\mu) \\ &\vdots \\ R_{p-1}(\mu) &= Q_p(\mu)R_p(\mu) + R_{p+1} \end{aligned} \quad (34)$$

Now g, R_1, R_2, . . . are polynomials of decreasing degrees in μ so that, after a finite number of steps, a remainder R_{p+1} is reached which is independent of μ. It can be shown that the condition that f and g have at least one common root is $R_{p+1} = 0$. Also, the common roots can be obtained from $R_p(\mu) = 0$.

Because $a_0, a_1, \ldots, a_m$ depend on α, R_{p+1} is a function of α and the flutter condition is $R_{p+1}(\alpha) = 0$. The values of α corresponding to flutter can thus be determined by the usual interpolation procedures. The associated values of μ follow from $R_p(\mu) = 0$.

By varying k, flutter boundaries in the α, μ plane can thus be obtained for specific values of M, L, s, g, ϵ_x, and ϵ_y.

Numerical Results and Discussion

In this section, numerical results are given for an array of panels with one or two panels in the chordwise direction.

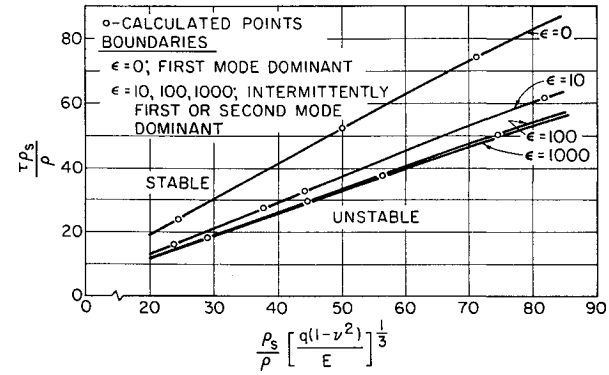

Fig. 3 Critical stability boundaries from four-mode analysis for flat panels with partially clamped edges, $M = 1.35$, $s = 0$, $g = 0.01$, $L = 1$.

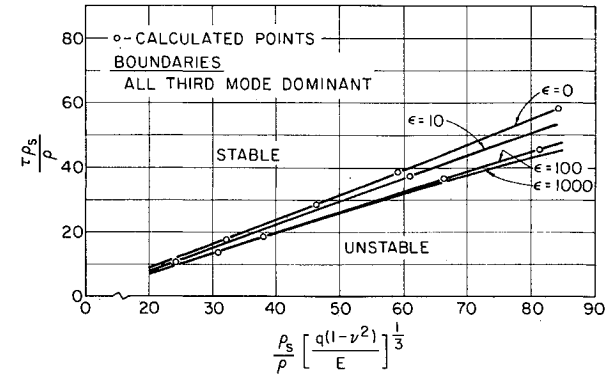

Fig. 5 Critical stability boundaries from four-mode analysis for flat panels with partially clamped edges, $M = 1.35$, $s = 1$, $g = 0.01$, $L = 1$.

Table 1 Flutter vector and reduced flutter frequency from four-mode analysis for flat panels with partially clamped edges: $M = 1.35$, $s = \frac{1}{4}$, $g = 0.01$, $L = 1$

ϵ	k	$\frac{\tau\rho_s}{\rho}$	$\frac{\rho_s}{\rho}\left[\frac{q(1-\nu^2)}{E}\right]^{1/3}$	q_1	θ_1	q_2	θ_2	q_3	θ_3	q_4	θ_4
0	0.70	60.64	79.192	0.1143	−3.2450	1	0	0.0463	−0.0089	0.0014	−0.0277
0	0.80	55.04	67.894	0.0970	−3.2766	1	0	0.0397	−0.0127	0.0011	−0.0590
0	1.00	41.06	48.039	0.0827	−3.3468	1	0	0.0351	−0.0313	0.0010	−0.1945
0	1.20	22.89	28.665	0.0996	−3.4121	1	0	0.0446	−0.0683	0.0017	−0.3769
0	1.25	16.95	22.738	0.1221	−3.4200	1	0	0.0551	−0.0803	0.0024	−0.4056
10	0.80	51.63	75.849	0.1130	−3.2528	1	0	0.0594	−0.0094	0.0027	−0.0325
10	0.90	46.40	65.270	0.0997	−3.2825	1	0	0.0530	−0.0144	0.0024	−0.0644
10	1.00	40.16	55.206	0.0932	−3.3137	1	0	0.0504	−0.0232	0.0023	−0.1143
10	1.20	24.42	34.937	0.1041	−3.3728	1	0	0.0588	−0.0538	0.0031	−0.2592
100	0.80	48.76	81.914	0.1368	−3.2352	1	0	0.0716	−0.0082	0.0039	−0.0250
100	1.00	39.90	61.698	0.1076	−3.2891	1	0	0.0577	−0.0174	0.0031	−0.0809
100	1.20	27.31	42.310	0.1080	−3.3448	1	0	0.0600	−0.0408	0.0036	−0.1944
100	1.30	19.01	31.385	0.1301	−3.3660	1	0	0.1420	−0.0616	0.0133	−0.2443
1000	0.80	48.19	83.071	0.1436	−3.2322	1	0	0.0723	−0.0083	0.0039	−0.0247
1000	1.00	39.87	63.050	0.1119	−3.2845	1	0	0.0576	−0.0166	0.0031	−0.0751
1000	1.10	34.38	53.549	0.1070	−3.3126	1	0	0.0560	−0.0255	0.0031	−0.1218
1000	1.20	27.96	43.953	0.1098	−3.3398	1	0	0.0585	−0.0384	0.0034	−0.1823

The chordwise deflection is approximated by using the first four chordwise mode shapes. Because L and m are small, the foregoing first procedure is applied to obtain the aerodynamic integrals in (18).

For the structural damping coefficient g, a value of 0.01 is chosen as representative of practical design configurations. Also, the rib and stringer restraint is chosen such that $\epsilon_x = \epsilon_y = \epsilon$.

Since the dynamic pressure q is a pertinent design parameter, it is perhaps appropriate to replace the speed of sound by $(q/\frac{1}{2}\rho M^2)^{1/2}$ in α. The flutter boundaries can then be given in the $\tau\rho_s/\rho$, $(\rho_s/\rho)[q(1-\nu^2)/E]^{1/3}$ plane.‡

In Fig. 2, the results of a typical calculation are given. By "first and second mode coupled" is meant that the first and second degrees of freedom in the flutter vectors are large, with the first degree of freedom dominating. The unstable regions are below the "first and second coupled" and "third mode dominant" boundary, between the "second mode dominant" and "second and first mode coupled," and within the "fourth mode dominant" boundary. The second mode dominant boundary is thus the most critical one. In succeeding figures only critical flutter boundaries are shown.

The effects of edge constraint and aspect ratio were studied by varying ϵ and s. In Figs. 3–5, the critical stability boundaries are given for $M = 1.35$, $g = 0.01$, $L = 1$, and $s = 0$, $\frac{1}{4}$, and 1, respectively. The Mach number $M = 1.35$ was chosen since the largest thickness ratio requirements to prevent flutter are usually found at this Mach number.[1] In each figure, the stable and unstable regions are indicated for $\epsilon = 0$, 10, 100, and 1000. As to be expected, an increase of the rib and stringer restraint has a stabilizing effect. However, this effect diminishes with increasing s (decreasing aspect ratio). Also, although at $s = 0$ the critical flutter boundaries are predominantly first-mode boundaries, at $s = \frac{1}{4}$ the boundaries are predominantly second and at $s = 1$, predominantly third-mode boundaries.

In Table 1,§ the flutter vectors corresponding to the calculated points in Fig. 4 are given. Note that the flutter vectors contain only one large generalized coordinate. The second largest normalized coordinate varies between 0.04 and 0.15 when the edge condition changes from pinned to clamped. Consequently, even for the clamped edge condition, the flutter boundaries in the region between Mach 1 and $2^{1/2}$ are nearly one degree-of-freedom boundaries.

To investigate the effect of Mach number on the critical stability boundary, the case $\epsilon = 100$, $s = 1$, $L = 1$, $g = 0.01$ was repeated for $M = 1.1$, 1.25, 1.5, and 2.0. The results are given in Fig. 6. It can be shown that the case $\epsilon = 100$ corresponds to a nearly clamped edge condition. It is seen that even at $s = 1$ the thickness ratio required to prevent flutter in the low supersonic region is about twice the thick-

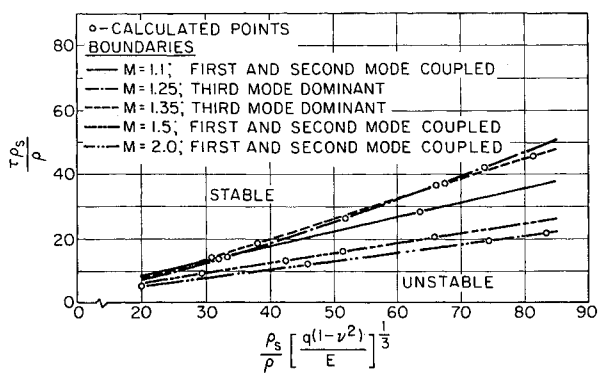

Fig. 6 Critical stability boundaries from four-mode analysis for flat panels with partially clamped edges, $s = 1$, $L = 1$, $g = 0.01$, $\epsilon = 100$.

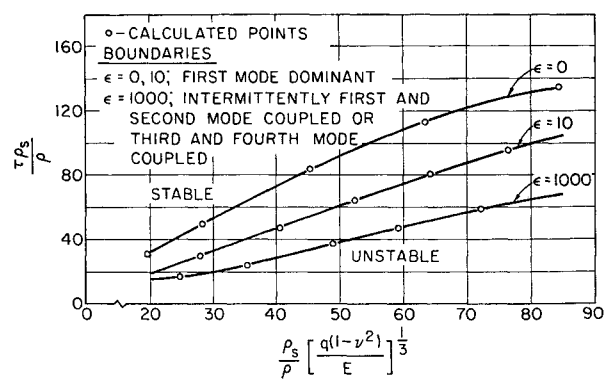

Fig. 7 Critical stability boundaries from four-mode analysis for flat panels with partially clamped edges, $M = 1.35$, $s = 0$, $g = 0.01$, $L = 2$.

‡ The parameter $[\rho_s/\rho][q(1-\nu^2)/E]^{1/3}$ is used here instead of the more familiar parameter $\tau[E/q(1-\nu^2)]^{1/3}$ to prevent the appearance of τ in both parameters.

§ The flutter vectors associated with the other figures are given in Ref. 7. They are omitted here to conserve space.

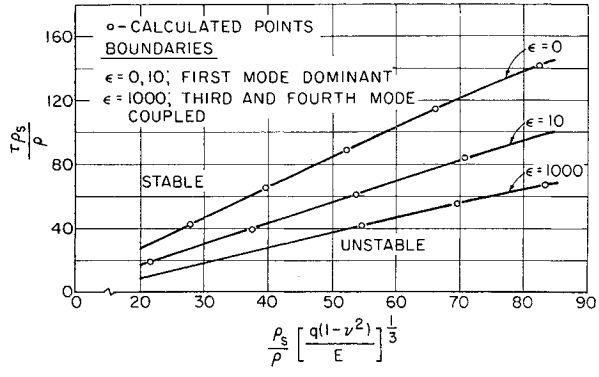

Fig. 8 Critical stability boundaries from four-mode analysis for flat panels with partially clamped edges, $M = 1.35$, $s = \frac{1}{4}$, $g = 0.01$, $L = 2$.

ness ratio required at the higher Mach numbers. Note that, at $M = 1.25$ and 1.35, the flutter vector has only the third generalized coordinate as a large coordinate. At $M = 1.1$, 1.5, and 2.0, coupling between the first and second generalized coordinates takes place.

The effects of edge constraint and aspect ratio for the configuration with two chordwise panels are shown in Figs. 7 and 8. It is instructive to remark that in this case the first and third modes are antisymmetric with respect to the middle stringer, whereas the second and fourth modes are symmetric. It is seen that, in general, the critical flutter vectors for $M = 1.35$, $L = 2$, and $s = 0$ and $\frac{1}{4}$, consist predominantly of the antisymmetric first and third modes. However, coupling between generalized coordinates increases considerably as edge conditions vary from pinned to clamped for both $s = 0$ and $\frac{1}{4}$. For the pinned condition ($\epsilon = 0$), the second largest normalized coordinate is about 0.05, and for $\epsilon = 10$, it varies between 0.15 and 0.25. For the nearly clamped condition ($\epsilon = 1000$), the two largest coordinates occur in almost equal proportion, indicating very strong coupling. This strong coupling occurs intermittently between the first and second and the third and fourth coordinates for $s = 0$. For $s = \frac{1}{4}$, the strong coupling occurs between the third and fourth coordinates.

The pronounced destabilizing effects of increasing the number of chordwise panels can be seen by comparing Figs. 7 and 8 with Figs. 3 and 4, respectively. The case $L = 2$ and $s = 1$ has not been examined, since it is expected, from the results for $L = 1$ in Fig. 5, that the fifth mode will dominate, and thus at least six degrees of freedom should be introduced.

References

[1] Zeydel, E. F. E., "Large deflection panel flutter," Air Force Office Scientific Research TN 1952 (January 1962).

[2] Lin, Y. K., "Free vibration of continuous skin-stringer panels," J. Appl. Mech. 82, 669–676 (1960).

[3] Miles, J. W., "Vibrations of beams on many supports," Proc. Am. Soc. Civil Engrs. 82, 1–9 (1956).

[4] Luke, Y. L. and St. John, A. D., "Supersonic panel flutter," Wright Air Development Center TR 57-252 (July 1957).

[5] Bromwich, T. J., *An Introduction to the Theory of Infinite Series* (MacMillan and Company, Ltd., London, England, 1949).

[6] Bôcher, M., *Introduction to Higher Algebra* (The MacMillan Company, New York, 1936), Chap. 67.

[7] Zeydel, E. F. E. and Kobett, D. R., "The flutter of flat plates with partially clamped edges in the low supersonic region," Air Force Office of Scientific Research TR Part I (January 1963).